Robust, Non-Linear Impedance Control for Robot Manipulators

H. Kazerooni
Mechanical Engineering Department
University of Minnesota
Minneapolis, MN, 55455

ABSTRACT

The work presented here is a practical, non-linear controller design methodology for robot manipulators that guarantees: 1)the robot end-point follows an input command vector "closely" when the robot is not constrained by the environment, and 2) the contact force is a function of the same input command vector (used in the unconstrained environment) when the robot is constrained by the environment. The controller is capable of "handling" both types (constrained and unconstrained) of maneuverings, and is robust to bounded uncertainties in robot dynamics. The controller does not need any hardware or software switch for transition between unconstrained and constrained maneuvering. In this design method, the structural compliancy of the manipulator has also been considered. A set of experiments were carried out to describe how this unified approach can develop electronic compliancy in a robot manipulator. The control architecture has been described by two different methods; frequency domain, and input/output time domain properties.(25,26)

Nomenclature

A	the closed-loop mapping from r to f
d	n×1 external-force vector on the robot end-point
e	n×1 input trajectory vector
e_m,d_m	positive scalars
E	environment dynamics
f	n×1 vector of the contact force
f_∞, y_∞	the limiting value of the contact force and robot position for rigid environment
G	robot dynamics with positioning controller
H	compensator transfer function matrix
r	n×1 input-command vector
n	degrees of the freedom of the system n<6
S	robot manipulator stiffness
T	positive scalar
V	the forward loop mapping from e to f
x	environment deflection
y	n×1 vector of the robot end-point position
X_o	n×1 environment-position vector before contact
θ	n×1 vector of the joint angles of the robot
ε_e, ε_d	positive scalars
ω_o	frequency range of operation (bandwidth)
α_i, β_i	positive scalars

1. Introduction

In general, manipulation consists of two categories. In the first category, the manipulator end-point is free to move in all directions. In the second, the manipulator end-point interacts mechanically with the environment. Most assembly operations and manufacturing tasks require mechanical interactions with the environment or with the object being manipulated, along with "fast" motion in free and unconstrained space. Therefore, the object is to develop a control system such that the robot will be capable of "handling" both types of maneuvers without any hardware and software switches. The hardware and software switches used in algorithms such as hybrid force/position control (20) develop unpleasant transient response in the transition period. In meeting the above objective, the goal is to develop a controller for the robot manipulator such that:

1) The robot end-point follows an input-command vector very "closely" when the robot is not constrained. (a more rigorous definition for "closely" will follow.)
2) The contact force is a function of the same input-command (used in the unconstrained maneuvering) when the robot is constrained by the environment.

Note that the above notation does not imply a force control technique (18,19,20,28). We are looking for a positioning controller that guarantees the tracking of the input-command vector when the robot is not constrained, as well as the relation of the contact-force vector with the same input-command vector when the robot encounters an unknown environment.

2. Motivation

The following scenario reveals the crucial need for compliance control in high-speed manufacturing operations. Consider an assembly operation by a human worker in which there are some parts to be assembled on the table. Each time the worker decides to reach the table and pick up a part, she/he always encounters the table with a non-zero speed; in other words she/he hits the table while picking up the parts. The worker also assembles the parts with a non-zero speed; meaning the parts hit each other while they are assembled. The ability of the human hand to encounter the unknown and unstructured environment with non-zero speed allows for a higher speed of operation. This ability in human beings flags the existence of a compliance control mechanism in biological systems. This mechanism guarantees the "stability" of contact forces in constrained maneuvering, in addition to high speed maneuvering in an unconstrained environment. With the

existing state of technology, we do not have an integrated robotic assembly system that can encounter an unstructured environment as a human worker can. No existing robotic assembly system is faster than a human hand. The compliancy in the human hand allows the worker to encounter the environment with non-zero speed. The above example does not imply that we choose to imitate human factory-level physiological/psychological behavior as our model to develop an over-all control system for manufacturing tasks such as assembly and finishing processes. We stated this example to show that: 1) a reliable and optimum solution for simple manufacturing tasks such as assembly does not yet exist and 2) it is the existence of an efficient, fast compliance control system in human beings that allows for superior and faster performance. We believe compliance control is one of the key issues in the development of high-speed manufacturing operations for robot manipulators.

The control method explained here is general and applies to all industrial and research manipulators. We describe the method in two different fashions. First we choose the conventional frequency domain approach for understanding the fundamentals of the control methodology (Sections 3-9). The convenient notation of Laplace and strong Nyquist criteria allow us to arrive at a fundamental condition for stability of the robot manipulator when it is in contact with the environment (in particular a hard environment in Section 8). In sections 10-13 we take the time-domain non-linear approach to arrive at the stability condition. The results of two approaches are similar.

3. The Controller Design Objectives

The design objective is to provide a stabilizing dynamic compensator for the robot manipulator such that the following design specifications are satisfied.

I. The robot end-point follows an input-command vector, r, for all $\omega \in (0,\omega_0)$ when the robot manipulator is free to move.

II. The contact force* is a function of the input command vector, r, for all $\omega \in (0,\omega_0)$ when the robot is in contact with the environment.

The first design specification allows for free manipulation when the robot is not constrained. If the robot encounters the environment, then according to the second design specification, the contact force will be a function of the input command vector. Thus, the system will not have a large and uncontrollable contact force. Note that r is an input command vector that is used for both unconstrained and constrained maneuverings. The end-point of the robot will follow r when the robot is unconstrained, while the contact force will be function of r (preferably a linear function for some bounded frequency range of r) when the robot is constrained.

* In this paper *force* implies force and torque and *position* implies position and orientation.

4) Dynamic Model of the Robot with Positioning Controllers in Frequency Domain

In this section we develop a new approach to describe the dynamic behavior of a large class of industrial and research robot manipulators having positioning controllers. We plan to model the dynamic behavior of these manipulators by a general mathematical form.

The fact that most industrial manipulators have some kind of positioning controllers is the motivation behind our approach. Also, a great number of methodologies exist for the development of the robust positioning controllers for direct and non-direct robot manipulators (23,24,27).

The end-point position of a robot manipulator that has a positioning controller is "approximately" equal to the vector of input trajectory, e, if e is bounded in magnitude and frequency. The approximate equality of e and the actual end-point position (in absence of external force on the robot end-point) can be represented by inequality 1:

$$\frac{\| y(j\omega,e,\theta) - e(j\omega) \|_2}{\| e(j\omega) \|_2} \leq \varepsilon_e \quad \text{for all } \omega \in \omega_0 \text{ and } \|e\|_2 \leq e_m \quad (1)$$

where ω_0 and e_m are finite scalars; and θ represents the configuration of the robot manipulator. ($\|.\|_2$ denotes the Euclidean norm.) e and y are the n-dimensional ($n \leq 6$) vector of input trajectory and end-point position in a global cartesian.

Since the dynamic behavior of robot manipulators with positioning controllers in general is considered non-linear, the amplitude of the output position, y, depends not only on the amplitude of the input trajectory, e, but also on the orientation of the robot, θ.

Some explanations are needed for the practical conditions that are imposed by e_m and ω_0 on inequality 1. Because of the limitation on the size of the actuator torque, one cannot track a "large" trajectory vector, e, with a small tracking error, ε_e, within the frequency range of $(0,\omega_0)$. Scalar e_m is defined to represent the confinement of the magnitude of e. Physical systems are not responsive to high frequency input trajectories. Inequality 1 will not hold at high frequencies. ω_0 is introduced to represent this limitation. The frequency range $(0,\omega_0)$ where inequlity 1 holds, is called the bandwidth of the closed-loop tracking system (1,5,9). ε_e is a small number for good positioning systems. As an example, for the ADEPT robot, ε_e is equal to 0.01 for all $\|e\|_2 \leq 1$ cm, and $\omega \in (0, 5$ hertz).

Note that we chose the frequency domain to represent the dynamic behavior of the closed-loop positioning robot. This allows us to represent an approximation of the dynamic behavior of the closed-loop positioning robot without being specific about the nature of the input trajectory, e, and the structure of the positioning controller. For any manipulator, with any type of positioning controller, one can always arrive at inequality 1 experimentally or analytically. Conservative values for ω_0 and e_m are adequate to represent an approximation of the closed-loop positioning dynamic for the robot. We define a transfer function matrix to alter inequality 1 to an

equality as given by equation 3.

$$y(j\omega,e,\theta)=G(j\omega,e,\theta)\, e(j\omega) \qquad (3)$$

where:

$$\frac{\| (G(j\omega,e,\theta) - 1_n)\, e(j\omega)\|_2}{\| e(j\omega)\|_2} < \varepsilon_e \text{ for all } \omega\in\omega_0 \text{ and } \|e\|_2 < e_m \qquad (4)$$

Readers can think of $G(j\omega,e,\theta)$ as a describing function matrix that maps the amplitude of the input trajectory, e to the amplitude of the robot position, y. For simplicity and generality of the figures for various concepts we drop the arguments of variables in the figures.

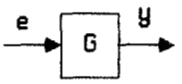

Figure 1: Input/Output Relationship for a Robot with a Positioning Controller

We plan to arrive at a dynamic compensator which develops compliancy for the robot manipulator in the global cartesian coordinate frame. Since this compensator will be independent of the structure of G, one need not be concerned with the "details" of G. We prefer equality 3 (when inequality 4 holds) to inequality 1 because of its convenience in notation. G is a transfer function matrix that maps the amplitude of the input trajectory to the amplitude of the actual robot position such that inequality 4 (and consequently inequality 1) is true.

Robot manipulators with positioning controllers are not infinitely stiff in response to external forces (also called disturbances). Even though the positioning controllers of robots are usually designed to follow the input trajectory (according to inequlity 1) and reject disturbances, the robot end-point moves "somewhat" in response to imposed forces on the robot end-point. The motion of the robot end-point in response to imposed forces is due to either structural compliance in the robot or the positioning controller compliance. The motion of the robot manipulator in response to the external forces can be defined similarly by a transfer function mstrix similar to equation 3. The motion of the end-point of a robot under the imposed force, d, at the end-point, in the absence of any input trajectory can be depicted by the block diagram in Figure 2 and equation 5 such that inequality 6 is satisfied.

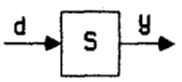

Figure 2: External Force/Output Relationship for Robot with a Positioning Controller

$$y(j\omega,d,\theta)=S(j\omega,d,\theta)\, d(j\omega) \qquad (5)$$

$$\frac{\| S(j\omega,e,\theta)\, d(j\omega)\|_2}{\| d(j\omega)\|_2} < \varepsilon_d \text{ for all } \omega\in\omega_0 \text{ and } \|d\|_2 < d_m \qquad (6)$$

$d(j\omega)$ is an n-dimensional vector of the external force that is imposed on the robot end-point. S is a transfer function matrix that represent the compliance (1/stiffness) of the robot. S is called the sensitivity matrix and for "good" positioning systems is quite "small". (By "small" we mean the maximum singular value* of S is a small number for all the frequencies that the external force, d, affect the system.)

Assuming that the effect of d and e can be added linealrly, equation 7 represents the dynamic behavior of a robot with a positioning controller:

$$y(j\omega,d,\theta)= G(j\omega,e,\theta)e(j\omega)+S(j\omega,d,\theta)\, d(j\omega) \qquad (7)$$

where G and S are given by equations 4 and 5. Figure 3 shows the complete dynamic behavior of the robot manipulator with a positioning controller.

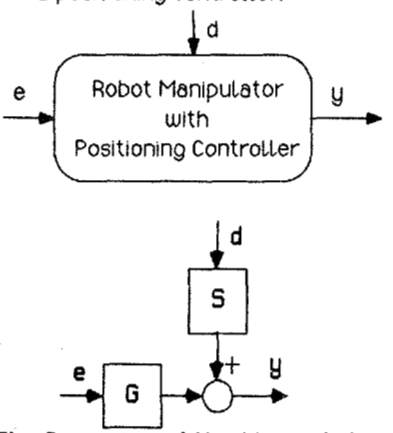

Figure 3: The Dynamics of the Manipulator with Positioning Controller

We deal with the robustness at this stage. One can design a positioning compensator to develop a tracking system such that the closed-loop system is always robust to the bounded uncertainties in the open loop dynamics of the robot. It is clear that the more uncertain the model of the robot is, the smaller bandwidth (slower response) can be achieved for the tracking system. On the other hand, if very little uncertainties is allowed in modelling the open loop dynamics of the robot manipulator, a wide (and consequently fast) tracking system can be developed for the system. (5)

5. Environment Dynamics in Frequency Domain

There is no specific model for the environment dynamics. The environment can be very "soft" or very "hard". We do not restrain ourselves to any geometry or to any structure. We can assume that if one point on the surface of environment is displaced (e.g. by the end-point of the robot) as vector of x, then the required force to do such a task is defined by f (Figure 4).

$$f(j\omega,x) = E(j\omega,x)\, x(j\omega) \qquad (8)$$

* The maximum singular value of H is defined as:

$$\sigma_{max}(H) = \max \frac{\| H\, r\|_2}{\| r\|_2}$$

Where $r=0_n$ and $\|.\|_2$ denotes the Euclidean norm.

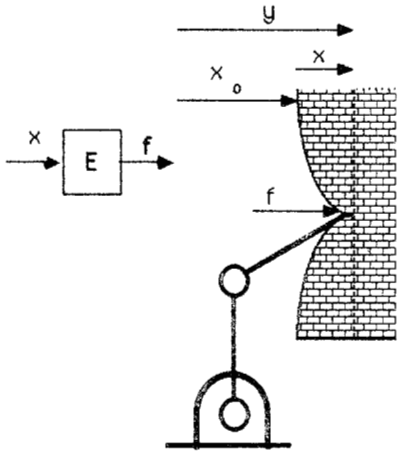

Figure 4: The Environment and its Dynamics

x_0 is the initial location of the point of contact before deformation occurs and y is the robot end-point position. ($x=y-x_0$). $E(j\omega,X)$ is a complex matrix that maps the amplitude of the displacement vector, x to the amplitude of the contact force, f. The matrix E is a n×n transfer function matrix. No assumption about E is made; E is a sigular matrix when the robot interacts with the environment in some directions only. For example, in grinding a surface, the robot is constrained by the environment in the direction normal to the surface only. Readers can be convinced of the truth of equation 8 by analyzing the relationship of the force and displacement of a spring as a simple model of the environment. E resembles the stiffness of a spring.

6. Dynamic Behavior of the Robot and Environment

Suppose a manipulator with dynamic equation 7 is in contact with an environment given by equation 8. The contact force will be equal to f. Note that when the robot manipulator and environment are in contact with each other, $f=-d$ and $x=y-x_0$. Combining equations 7 and 8, equation 9 is derived to describe the dynamic behavior of the robot and the environment. (For simplicity in notation the arguments of functions are omitted.)

$$y = (I + S E)^{-1} G e \qquad (9)$$

Figure 5 shows the robot manipulator and the environment when they are in contact with each other. Note that in some applications, the robot will only have uni-directional force on the environment. For example, in the grinding of a surface by a robot, the robot can only push the surface. If we consider positive f_i for "pushing" and negative f_i for "pulling", then the robot manipulator and the environment are in contact with each other along those directions where $f_i>0$ for i=1,...,n. On the other hand, in some applications such as screwing a bolt, the interaction force can be positive and negative. This means the robot can have clockwise and counter clockwise interaction torque. The non-linear discriminator block-diagram in Figure 5 is drawn with dashed-line to illustrate the above concept.

When the robot is not in contact with the environment, then E=0 and the equation that governs the dynamics of the system is given by equation 10 (the same as equation 3).

$$y = G e \qquad (10)$$

Note the natural feedback in the system; the force developed in the system due to the interaction of the robot manipulator and the environment affects the robot motion in a feedback fashion.

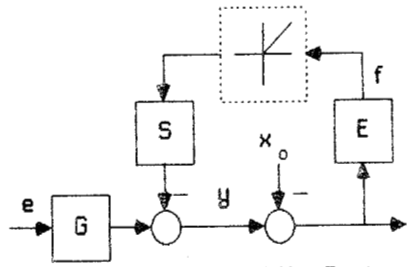

Figure 5: The Manipulator and the Environment

7. The Closed-Loop Architecture

The control architecture in Figure 6 shows how compliancy is being developed in the system. $H(j\omega)$ is a compensator to be designed. The input to this compensator is the contact force. The compensator output signal is being subtracted from the vector of the input command, r, resulting in the error signal, e as the input trajectory for the robot manipulator.

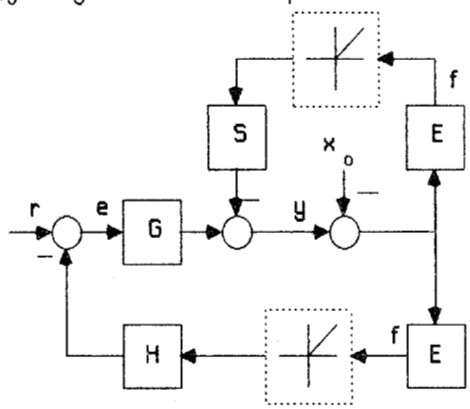

Figure 6: The Closed-Loop System

There are two feed-back loops in the system; the upper loop (which is the natural feedback loop), is the same as the one shown in Figure 5. This loop shows how the contact force affects the robot in a natural way when the robot is in contact with the environment. The lower feedback loop is the "controlled" feedback loop. We chose this architecture in the presentation of the system to emphasize the separation of the two loops. If the robot and the environment are not in contact, then the block diagram reduces to the one shown in Figure 3, which is a simple positioning system. When the robot and the environment are in contact, then the value of the contact force and the end-point position of robot are given by equations 11 and 12 respectively.

$$f = E(I + SE + GHE)^{-1} Gr \quad (11)$$

$$y = (I + SE + GHE)^{-1} Gr \quad (12)$$

We plan to choose a class of compensators, H, to shape the impedance of the system in equation 11. This compensator must also guarantee the stability of the closed-loop system shown in Figure 6. When the system is not in contact with the environment, the actual position of the robot end-point is almost equal to the input trajectory governed by equation 3. When the system is in contact with the environment, then the contact force is a function of r according to equation 11. The input command vector, r, is used differently for the two categories of maneuverings; as a trajectory command in unconstrained space (equation 3) and as a command to shape the force in constrained space, (equation 11). We do not command any set-point for force as we do in admittance control or in a force control system (20). This method is called Impedance Control (2,3,4,6,7) because it accepts a position vector as the input and it reflects a force vector as output. There is no hardware or software switch in the control system when the robot travels from unconstrained space to constrained space. The feedback loop on the contact force closes naturally when the robot encounters the environment.

8. Very Rigid Environment

In most manufacturing tasks such as robotic deburring (8,12,13,14,15), the end-point of the robot manipulator is in contact with a very stiff environment In this section, we plan to calculate the limiting value for f and y when the robot manipulator and a very rigid environment are interacting with one another. According to the results in Appendix B, when the environment is very stiff, (E approaches ∞ in the singular value sense), the resulting value for the contact force and the end-point position are given by equations 13 and 14 respectively:

$$f_\infty = (S+GH)^{-1} G r \quad (13)$$

$$y_\infty = 0 \quad (14)$$

Since $G \approx I_n$ for all $\omega \in (0,\omega_0]$, the value of the contact force, f, within the bandwidth of the system $(0,\omega_0]$ can be approximated by equation 15:

$$f_\infty \approx (S+H)^{-1} r \qquad \text{for all } \omega \in (0,\omega_0] \quad (15)$$

The fact that most tracking systems follow their commands very closely within their bandwidths is the motivation to consider $G \approx I_n$. By knowing S and choosing H, one can shape the impedance of the system. If H is chosen such that (S+H) is "large" in the Singular Value sense at high frequencies, then the contact force in respose to high frequency components of r will be small. The value of (S+H) within $(0,\omega_0]$ is the designer's choice and, depending on the task, it can have various values in different directions (6,7,10,11,22). A small value for $(S+H)^{-1}$ within $(0,\omega_0]$ develops a compliant system while a large $(S+H)^{-1}$ generates a stiff system.

By specifying H, the designer governs the behavior of the system in constrained maneuvers. Large members of the matrix $(S+H)^{-1}$ imply large interaction forces and torques. Small memebers of the matrix $(S+H)^{-1}$ allow for a considerable amount of compliancy in the system. $(S+H)^{-1}$ in one sense represents the type of behavior a designer may wish a stable positioning system to exhibit. For example, if the system is expected to encounter some physical constraint in a particular direction, H may be selected such that contact force is ensured in that direction. Therefore $(S+H)^{-1}$ can be formed to contain values appropriate for different directions.

9. Stability of the Closed-Loop System

The objective of this section is to arrive at a sufficient condition for stability of the system shown in Figure 6. This sufficient condition automatically leads to the introduction of a class of compensators, H, that can be used to develop compliancy for the class of robot manipulators that have positioning controllers. The detailed derivation for the stability condition is given in Appendix A. According to the results of Appendix A, the sufficient condition for stability is given by inequality 16:

$$\sigma_{max}[GHE] < \sigma_{min}[SE + I_n] \quad \text{for all } \omega \in (0,\infty) \quad (16)$$

or equivalently,

$$\sigma_{max}[H] < \frac{1}{\sigma_{max}[E(SE + I_n)^{-1}G]} \quad \text{for all } \omega \in (0,\infty) \quad (17)$$

If H is chosen outside of this class, instability and consequent separation may occur. (Inequality 17 is a sufficient condition for stability. If inequality 17 is not satisfied, no conclusion on the stability of the system can be achieved.) $E(SE+I_n)^{-1}G$ is the forward loop transfer function of the system in Figure 7. According to inequality 16, the "size" of H in all directions must be smaller than the reciprocal of the maximum "size" of the forward loop transfer funtion, $E(SE+I_n)^{-1}G$. Note that S and E are functions of their inputs. One must find the largest value of the maximum singular value of $E(SE+I_n)^{-1}G$ as the most conservative case. Inequality 16 guarantees the stability of the system if the maximum singular value of H is chosen to be less than the reciprocal of the maximum singular value of $E(SE+I_n)^{-1}G$ for all possible inputs, r and robot orientation, θ.

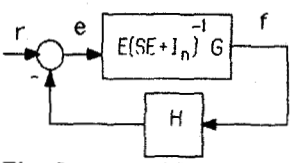

Figure 7: The Simplified Form of Figure 6

Inequality 17 reveals some facts about the size of H. The smaller the sensitivity of the robot manipulator is, the smaller H must be chosen. Also from inequality 17, the more rigid the environment is, the smaller H must be chosen. In the "ideal case", no H can be found to allow a perfect positioning system (S=0) to interact with an infinitely rigid environment (E=∞).

Stability for very rigid environment. If H is chosen to

guarantee the compliance in the system when the environment is infinitely rigid, then it must also satisfy the stability condition. Considering inequality 17, it can be shown that the stability criteria for interaction with a very rigid environment (when E approaches ∞ in the singular value sense) is given by inequality 18:

$$\sigma_{max}[H] \leq \frac{1}{\sigma_{max}[S^{-1}\ G]} \quad \text{for all} \quad \omega\in[0,\infty) \qquad (18)$$

It is clear that if the environment is very rigid, then one must choose a very small H to satisfy the stability of the system when S is "small". (A good positioning system has "small" S). Since $G\approx I_n$ for all $\omega\in[0,\omega_0]$, the bound for H, for a rigid environment and a "small" stiffness, is given by inequality 19.

$$\sigma_{max}[H] \leq \sigma_{min}(S) \quad \text{for all} \quad \omega\in[0,\omega_0] \qquad (19)$$

Inequality 19 states that one must at least have some compliancy inthe system to guarantee the stability. This compliancy can be provided by considering a passive compliant element in the robot (for example in the wrist). Practitioners have always observed that if there is some passive compliant elements between the robot and the environment, theα range of the stability will be much larger. Inequality 19 clearly shows the large value for S develops more range for stability for the closed-loop system.

Stability Condition when n=1. In the case of the one degree of freedom system (an example is given in Figure 10) the condition for stability is given by inequality 20.

$$|HG| < |(S+1/E)| \quad \text{for all} \quad \omega\in[0,\infty) \qquad (20)$$

$|.|$ denots the magnitude of the complex variable. Since in many cases $G\approx 1$ for all $0<\omega<\omega_0$, then H must be chosen such that the following inequality is satisfied.

$$|H| < |(S+1/E)| \quad \text{for all} \quad \omega\in[0,\omega_0] \qquad (21)$$

Equation 21 clearly shows that the more rigid the environment is, the smaller H must be chosen to guarantee stability. In the case of a rigid environment ("large" E) and a "good" positioning system ("small" S), H must be chosen as a very small gain.

10. Non-Linear, Time-Domain Dynamic Model of the Robot Manipulator with Positioning Controller

In sections 10-13 we take the time-domain non-linear approach to analyze the control architecture that was given in Figure 6. The general form of the dynamic behavior of the robot manipulator and the environment are given in sections 10-13. Section 13 describes the non-linear stability condition which confirms the results of Section 9.

The general form of the non-linear dynamic equations of a robot manipulator with positioning controller can be given by two non-linear vector functions G and S in equation 22.

$$y = G(e) + S(d) \qquad (22)$$

$$\text{where:} \quad \frac{\|y-e\|_p}{\|e\|_p} < \varepsilon_e \quad \text{for} \quad \|e\|_p \leq e_m \qquad (23)$$

$$\text{and:} \quad \frac{\|y\|_p}{\|d\|_p} < \varepsilon_d \quad \text{for} \quad \|d\|_p \leq d_m \qquad (24)$$

where y, G(e) and $S(d)\in\mathbb{R}^n$

(The definition for $\|.\|_p$ is given in Appendix C.) We purposely choose notations S and G for these mappings to remind the readers that the vector functions in equation 22 carry the same mappings that matrices G and S do in the frequency domain case of Section 4 (equation 7). Figure 3 shows the nature of mapping in equation 22. No assumption on the internal structure of G(e) and S(e) are made. We assume that G(e) and S(d) are stable non-linear operators in the L_p-space; in other words G(e) and S(d) are such that $G: L_p^n \rightarrow L_p^n$, $S: L_p^n \rightarrow L_p^n$ and also there exit constants α_1, β_1, α_2 and β_2 such that $\|G(e)\|_p < \alpha_1\|e\|_p + \beta_1$ and $\|S(d)\|_p < \alpha_2\|d\|_p + \beta_2$. (The definition for L_p-stability is given in Appendix C)

11. Non-Linear, Time-Domain Dynamic Behavior of the Environment

The dynamic behavior of the environment is given by a non-linear vector function E: $x\mapsto f$ where x and f are defined in Section 5.

$$f=E(x) \qquad (25)$$

No assumption is made on the structure of E. We also assume E is stable in L_p-sense; $E: L_p^n \rightarrow L_p^n$ and also there exit constants such as α_3 and β_3 such that $\|E(x)\|_p < \alpha_3\|x\|_p + \beta_3$. Here again we choose the same notation for this non-linear mapping as we did in the linear case. E in Section 5 is defined as a matrix for a linear transformation while in the general case, it is a stable non-linear vector function. Figure 4 shows mapping 25.

12. Non-Linear Dynamic Behavior of the Robot Manipulator and Environment

Combining equations 22 and 25 results in equation 26 which is the entire non-linear dynamic behavior of the manipulator and environment when they are in contact with one another. Note that again $x=y-x_0$ and $f=-d$.

$$y = G(e) - S(f) \qquad (26)$$

$$f=E(y-x_0) \qquad (27)$$

The block diagram in Figure 5 shows the nature of mappings 26 and 27. We define V as a mapping from e to f. In other words the mappings given by equations 26 and 27 can be simplified by mapping $V: e\mapsto f$. e and f are shown in Figure 8. (V is similar to $E(SE+I_n)^{-1}G$ in Figure 7.

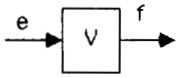

Figure 8: The Mapping from the Input Trajectory to the Contact Force

Note that we assume V is as stable operator in L_p-sense; in other words: $V: L_p^n \rightarrow L_p^n$ and also $\|V(e)\|_p < \alpha_4 \|e\|_p + \beta_4$ where α_4 and β_4 are constants.

13. Stability of the Closed-Loop System

The objective of this section is to arrive at a sufficient condition for stability of the system shown in Figure 9. The measured contact force is subtracted from the input-command vector, r as in Figure 9. This sufficient condition automatically leads to the introduction of a class of compensators, H, that can be used to develop compliancy for the class of robot manipulators that have positioning controllers. The following theorem states the stability condition of the closed-loop system shown in Figure 9. A corollary is given to represent a bound on H to guarantee the stability of the system. This corollary confirms the results of section 9.

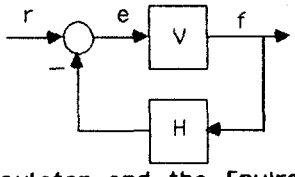

Figure 9: Manipulator and the Environment with Force Compensator, H (Simplified Version of Fig. 6)

I. If V is a L_p-stable operator, that is

a) $V(e): L_p^n \rightarrow L_p^n$ (28)

b) $\|v(e)\|_p < \alpha_4 \|e\|_p + \beta_4$ (29)

where α_4 and β_4 are positive constants, and if,

II. H is chosen as stable linear transfer function matrix such that mapping HV(e) is still L_p-stable, that is

a) $HV(e): L_p^n \rightarrow L_p^n$ (30)

b) $\|HV(e)\|_p < \alpha_5 \|e\|_p + \beta_5$ where $\alpha_5 < 1$ (31)

then the closed-loop system is L_p-stable. Condition I is already assumed in Section 12. The Proof is given in Appendix C.

Corollary

The key parameter in the theorem is the size of α_5. According to the above theorem, to guarantee the closed-loop stability of the system, H must be chosen such that the norm of HV(e) is linearly bounded with a slope that is smaller than unity. Considering inequality 29 , inequality 32 is true.

$$\|HV(e)\|_p < \|H\|_P [\ \alpha_4 \|e\|_p + \beta_4\ ] \quad (32)$$

Comparing inequality 31 and inequality 32, to guarantee the stability of the system, $\|H\|_P \alpha_4$ must be smaller than unity, or, equivalently:

$$\|H\|_P < 1/\alpha_4 \quad (33)$$

Substituting for α_4 from inequality 29:

$$\|H\|_P < 1/\alpha_4 < \frac{\|e\|_P}{\|V(e)\|_P - \beta_4} \quad (34)$$

To guarantee the stability of the closed-loop system, H must be chosen such that:

$$\|H\|_P < \frac{\|e\|_P}{\|V(e)\|_P} \quad (35)$$

Inequality 35 states that the L_p-norm of H must be less than the reciprocal of the "magnitude" of the mapping in the forward loop in Figure 9. This guarantees the stability of the closed-loop system. This result is a general form of the result which is given by inequality 17.

14. Experiments

A simple experiment is described here to show how impedance control can be employed to develop compliancy on a one degree of freedom system. A more practical example is given in reference 14. This experiment also points out the difference between employing impedance control [2,3,4,6,7,10,11] and admittance control in constrained maneuvers. The system consists of a link which is driven by a DC motor as shown in Figure 10. The DC motor has a positioning controller. This controller guarantees that the end-point of the link follows the trajectory command very closely. In this section, we are interested in observing the transient behavior of the link from unconstrained maneuvers to constrained maneuvers. The system is controlled according to Figure 6. A wide bandwidth force sensor is mounted on the link to measure the contact force. The controller is able to accept the value of the compensator, H in addition to the input-command vector, r. Several experiments were carried out on this set-up.

I. High-Speed Contact

In this experiment, the link is commanded to move beyond the solid block. As long as the link is not in contact with the aluminium block, the contact force is zero. After the link encounters the rigid block, the contact force rapidly increases to a finite value of one lb. Figure 11 shows the step-wise change of the force from zero to 1 lbf. The value of the force is proportional to the distance from the rigid block surface and the commanded position of the link. Equation 15 shows the proportionality of the contact force with the input command. After 1.25 seconds, the link is commanded to its original position step-wise. The contact force drops to zero. The over-shoot of the contact force shows the transient period.

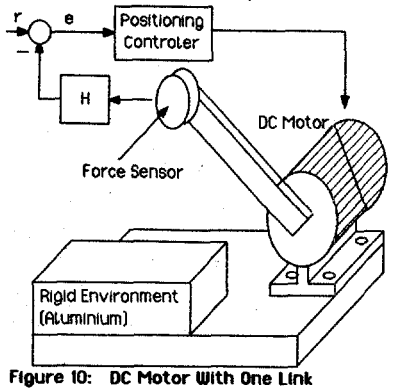

Figure 10: DC Motor With One Link

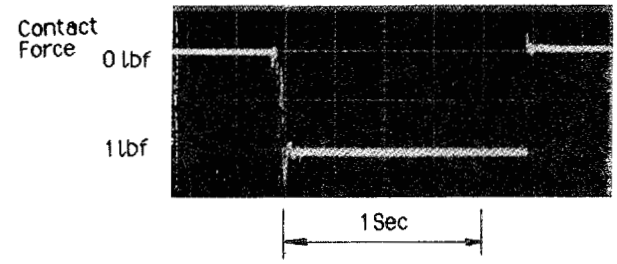

Figure 11: Experiment I

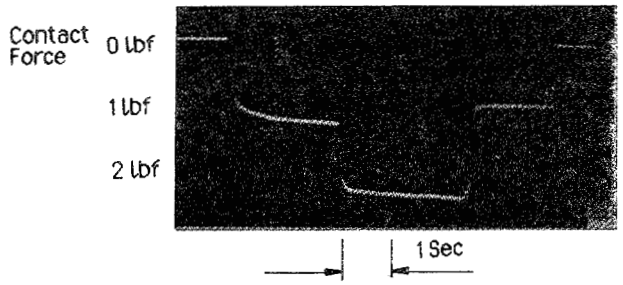

Figure 12: Experiment II

II. Step-Wise Change in Force During the Contact

This experiment shows the stability of the closed-loop system during the rapid change in the input command. In this experiment, the link is commanded to move beyond the surface of the solid block (Figure 12). The contact force is 1 lbf. After about 4 seconds, the link is commanded to move more. This increases the contact force to 2 lbf. The contact force is proportional to the commanded trajectory. After 5 seconds the link is commanded to move back. The force drops down to 0.8 lbs. After 1 second, the link is commanded to seperate the solid block. The force value drops down to zero.

III. Sinusoidal Contact Force

In this set of experiments, the link is commanded to follow a sinuousiodal trajectory while it is in contact with the solid object. Figure 13 shows the sinuousiodal contact force. The contact force is function of the input command trajectory.

Note that we have a positioning system for the DC motor and the link that has the ability to modulate the impedance of the system. It accepts a position vector, r, and it reflects a force as output. We do not command any set-point force as we do in admittance control. By assigning various position commands and by maintaining complete control on the value of H we can keep the contact force in a desired range.

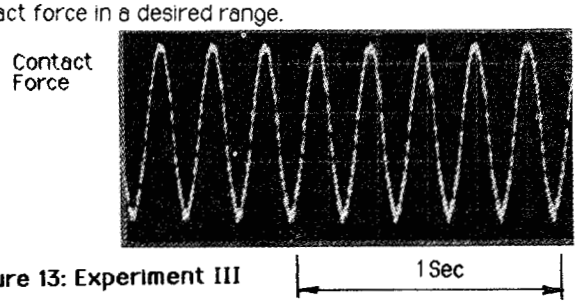

Figure 13: Experiment III

15. Summary and Conclusion

Manipulation requires interaction with the environment or with the object being manipulated. This paper presents a controller architecture for the robot manipulators that can generate electronic compliancy. We started with modeling the class of robot manipulators that have positioning controllers. This model is independent of the structure of the positioning controller of the robot manipulator. Having the robot and environment modeled in a very general form, we arrive at a new architecture control to guarantee electronic compliancy for the robot manipulators. This approach allows not only for tracking the input-comand vector, but also for compliancy in the system. The bound for the global stability of the manipulator and environment has been derived. A set of experiments have been conducted to verify the results.

Appendix A

The objective is to find a sufficient condition for stability of the closed-loop system in Figure 6. The block diagram in Figure 6 can be reduced to the block diagram in Figure A1 providing G^{-1} exists.

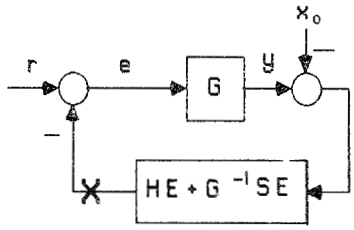

Figure A1: Simplified Block-Diagram of Figure 6

There are two elements in the feedback loop; HE and $G^{-1}SE$. $G^{-1}SE$ shows the natural force feedback while HE represents the controlled force feedback in the system. If H=0, then the system in Figure A1 reduces to the system in Figure 5 (a stable positioning robot manipulator which is in contact with the environment E.) The objective is to use Nyquist Criteria (17, 21) to arrive at the sufficient condition for stability of the closed system when H≠0. The following conditions are regarded:

1) The closed loop system in Figure A1 is stable if H=0. This condition simply states the stability of the robot manipulator and environment when they are in contact. (Figure 5 shows this configuration.)

2) H is chosen as a stable linear transfer function matrix. Therefore the augmented loop transfer function (GHE+SE) has the same number of unstable poles that SE has. Note that in many cases SE is a stable system.

3) Number of poles on $j\omega$ axis for both loop SE and $G(HE+G^{-1}SE)$ are equal.

Considering that the system in Figure A1 is stable when H=0, we plan to find how robust the system is when the term HE is added to the feedback loop. If the loop transfer function $G(G^{-1}SE)$ (without compensator, H) develops a stable closed-loop system, then we are looking for a condition on H such that the augmented loop transfer function $G(HE+G^{-1}SE)$ guarantees the stability of the

closed-loop system. According to the Nyquist Criteria, the system in the Figure A1 remains stable if the clockwise encirclement of the det.$[SE+GHE+I_n]$ around the center of the S-plane is equal to the number of unstable poles of the loop transfer function $[SE+GHE]$. According to conditions 2 and 3, the loop transfer functions SE and $(SE+GHE)$ both have the same number of unstable poles. The closed-loop system when H=0 is stable according to condition 1; the encirclements of det.$(SE+I_n)$ is equal to unstable poles of SE. When H is added to the system, for stability of the closed-loop system, the number of the encirclements of det.$(SE+GHE+I_n)$ must be equal to the number of unstable poles of the $(SE+GHE)$. Since the number of unstable poles of $(SE+GHE)$ and SE are the same, therefore for stability of the system det.$(SE+GHE+I_n)$ must have the same number of encirclements that det.$(SE+I_n)$ has. To guarantee the equality of the number of encirclements of det.$(SE+GHE+I_n)$ and det.$(SE+I_n)$, therefore det.$(SE+GHE+I_n)$ must not pass through the origin of the s-plane or equivalently:

$$\det.\,[SE+GHE+I_n] \neq 0 \qquad \text{for all } \omega\in(0,\infty) \qquad (A1)$$

A sufficient condition to guarantee that $\det.\,[SE+GHE+I_n]$ is not equal to zero is given by inequlity A2.

$$\sigma_{max}[GHE] < \sigma_{min}(SE+I_n) \qquad \text{for all } \omega\in(0,\infty) \qquad (A2)$$

$$\sigma_{max}[H] < \frac{1}{\sigma_{max}[E\,(SE+I_n)^{-1}\,G]} \qquad \text{for all } \omega\in(0,\infty) \qquad (A3)$$

Note that $E(SE+I_n)^{-1}G$ is the tranfer function matrix that maps e to the contact force, f. According to the result of the theorm, H must be chosen such that the size of H is smaller than the reciprocal of the size of the forward loop transfer function, $[E\,(SE+I_n)^{-1}\,G]$.

Appendix B

A very rigid environment generates a very large force for a small displacement. We choose the maximum sigular singular of E to represent the size of E. The following theorem states the limiting value of the force when the robot manipulator is in contact with a very rigid environment.

Theorem

If $\sigma_{min}(E)>M$, where M is an arbitrarily large number, then the value of the force given by equation 11 will approach to the expression given by equation B1

$$f_\infty = (S+GH)^{-1}G\,r \qquad (B1)$$

Proof. We will prove that $\sigma_{max}(f_\infty - f)$ approaches a small number as M approaches a large number.

$$f_\infty - f = (S+GH)^{-1} \quad [\,I_n - (S+GH)\,E\,(I_n+SE+GHE)^{-1}\,]\;Gr \qquad (B2)$$

Factoring $(I_n+SE+GHE)^{-1}$ to the right hand side:

$$f_\infty - f = (S+GH)^{-1}\,(I_n+SE+GHE]^{-1}\,Gr \qquad (B3)$$

$$\sigma_{max}(f_\infty - f) < \sigma_{max}[S+GH]^{-1}\;\sigma_{max}[I_n+SE+GHE]^{-1}\;\sigma_{max}[G] \qquad (B4)$$

$$\sigma_{max}(f_\infty - f) < \frac{\sigma_{max}[G]}{\sigma_{min}[S+GH]\;(\;\sigma_{min}[SE+GHE]-1\;)} \qquad (B5)$$

$$\sigma_{max}(f_\infty - f) < \frac{\sigma_{max}[G]}{\sigma_{min}[S+GH]\;(\;\sigma_{min}[S+GH]\;\sigma_{min}[E]-1\;)} \qquad (B6)$$

$\sigma_{max}[G]$ and $\sigma_{min}[S+GH]$ are bounded values. If $\sigma_{min}[E]>M$, then it is clear that the left hand side of inequality B6 can be arbitrarily small number by choosing M to be a large number. The proof for $y_\infty \approx 0$ is similar to the above.

Appendix C

Definitions 1 to 5 will be used in proof of the stability of the closed-loop system [25,26].

Definition 1: For all $p\in[1,\infty)$, we label as L^n_p the set consisting of all functions $f=[f_1,f_2,\ldots,f_n]^T:[0,\infty)\rightarrow\mathbb{R}^n$ such that:

$$\int_0^\infty |f_i|^p\,dt < \infty$$

Definition 2: For all $T\in[0,\infty)$, the function f_T defined by:

$$f_T=\begin{cases} f & 0\leq t\leq T \\ 0 & T<t \end{cases}$$

is called the truncation of f to the interval [0,T].

Definition 3: The set of all functions $f=[f_1,f_2,\ldots,f_n]^T:[0,\infty)\rightarrow\mathbb{R}^n$ such that $f_T\in L^n_p$ for all T is denoted by L^n_{pe} although f by itself may or may not belong to L^n_p.

Definition 4: The norm on L_p^n is defined by:

$$\|f(.)\|_p = \left[\sum_{i=1}^{n}\|f_i(.)\|_p^2\right]^{1/2}$$

Definition 5: Let $V(e)$: $L^n_{pe}\rightarrow L^n_{pe}$. We say the mapping V is L_p-stable operator, if:

a) $V(e): L_p^n \rightarrow L_p^n$

b) $\|v(e)\|_p < \alpha_4\|e\|_p + \beta_4$, where α_4 and β_4 are positive constants. According to this definition first we assume the function maps from L^n_{pe} to L^n_{pe}. It is very clear that if one does not show that $V:L^n_{pe}\rightarrow L^n_{pe}$, therefore the satisfaction of condition (a) is impossible because L^n_{pe} contains L^n_p. Once the mapping from L^n_{pe} to L^n_{pe} is established, then we say that the system is L_p-stable if, whenever the input belongs to L^n_p, the resulting output belong belongs to L^n_p and moreover the norm of the output is no larger than than α_4 times the nrom of the input plus the constant β_4.

Proof of the stability theorm

Define the closed-loop mapping A:r$\rightarrow$e (Figure 6).

$$e=r-HV(e) \qquad (C1)$$

For each finite T, inequality C2 is true.

$$\|e\|_{pe} < \|r\|_{pe} + \|HV(e)\|_{pe} \qquad \text{for all } t\in(0,T] \qquad (C2)$$

Since HV(e) is L_p-stable. Therefore, inequality C3 is true.

$$\|e\|_{pe} < \|r\|_{pe} + \alpha_5\|e\|_{pe} + \beta_5 \qquad \text{for all } t\in(0,T] \qquad (C3)$$

$$\|e\|_{Pe} < \frac{\|r\|_{pe}}{1-\alpha_5} + \frac{\beta_5}{1-\alpha_5} \qquad \text{for all } t\in[0,T) \qquad (C4)$$

Inequality C4, shows that $e(\cdot)$ is bounded over $[0,T)$. Because this reasoning is valid for every finite T, it follows that $e(\cdot)\in L^n_{pe}$, i.e., that $A:L^n_{pe}\mapsto L^n_{pe}$. Next we show that the mapping A is L_p-stable in the sence of definition 5. Since $r\in L^n_p$, therefore $\|r\|_p<\infty$ for all $t\in[0,\infty)$, therefore inequality C5 is true.

$$\|e\|_p < \infty \qquad \text{for all } t\in[0,\infty) \qquad (C5)$$

Inequlity A5 implies e belongs to L_p-space whenever r belong to L_p-space. With the same reasoning from equations C1 to C5, it can be shown that inequality A6 is true.

$$\|e\|_p < \frac{\|r\|_p}{1-\alpha_5} + \frac{\beta_5}{1-\alpha_5} \qquad (C6)$$

Inequality C6 and C5 taken together, guarantee that the *closed-loop mapping A is* L_p*-stable.*

References

1) Doyle, J. C., Stein, G., "Multivariable Feedback Design: Concepts for a Classical/Modern Synthesis", IEEE Transaction on Automatic Control AC-26(1), February, 81.
2) Hogan, N., "Adaptive Control of Mechanical Impedance by Coactivation of Antagonistic Muscles", IEEE Transaction on Automatic Control AC-29(7), July, 1984.
3) Hogan, N. "Impedance Control of Industrial Robots", Journal of Robotics and Computer Integrated Manufacturing 1(1):97-113, 1984.
4) Hogan, N., "Impedance Control: An Approach to Manipulation, Part 1: Theory, Part 2: Implementation, Part 3: Applications", ASME Journal of Dynamic Systems, Measurement, and Control, 1985.
5) Kazerooni, H., Houpt, P. K., "On The Loop Transfer Recovery", International Journal of Control , Volume 43, Number 3, March 1986.
6) Kazerooni, H., Houpt, P. K., Sheridan, T. B., "Fundamentals of Robust Compliant Motion for Manipulators" ,IEEE Journal of Robotics and Automation , N2, V2, June 1986
7) Kazerooni, H., Houpt, P.K., Sheridan, T.B., "A Design Method for Robust Compliant Motion of Manipulators", IEEE Journal of Robotics and Automation ,N2, V2, June86.
8) Kazerooni, H., Bausch, J. J., Kramer, B., "An Approach to Automated Deburring by Robot Manipulators", ASME Journal of Dynamic Systems, Measurements and Control, December 1986.
9) Kazerooni, H., Houpt, P. K., Sheridan, T. B., "An Approach to Loop Transfer Recovery using Eigenstructure Assignment". In poceedings of the American Control Conference, June 1985, Boston.
10) Kazerooni, H., Houpt, P. K., Sheridan, T. B., "Robust Copmliant Motion for Manipulators" , In proceeding of the International Conference on Robotics and Automation , San Francisco, April 1986.
11) Kazerooni, H., Houpt, P. K., Sheridan, T. B., "Robust Design Method For Impedance control of Robot Manipulators" , In proceeding of the American Control Conference , Seattle, June 1986.
12) Kazerooni, H., Bausch, J. J., Kramer, B., "An approach to Robotic Deburring" , In proceeding of American Control Conference , Seattle, June 1986.
13) Kazerooni, H. "Automated Robotic Deburring Using Electronic Compliancy; Impedance Control", In poceedings of the IEEE International Conference on robotics and Automation, Raleigh,North Carolina, April87.
14) Kazerooni, H., Guo, J., "Design and Construction of an Active End-Effector", IEEE In poceedings of the IEEE International Conference on Robotics and Automation, Raleigh, North Carolina, April 1987, and also IEEE Journal of Robotics and Automation.
15) Kramer, B., Bausch, J., Kazerooni, H.,"Compliant Tool Holders for Robotic Deburring", ASME Winter Annual Meeting, December 1986.
16) Lancaster, P., Lambda-Matrices and Vibrating Systems. Pergamon Press, 1966.
17) Lehtomaki, N. A., Sandell, N. R., Athans, M., "Robustness Results in Linear-Quadratic Gaussian Based Multivariable Control Designs", IEEE Transaction on Automatic Control AC-26(1):75-92, February, 1981.
18) Mason, M. T., "Compliance and Force Control for Computer Controlled Manipulators", IEEE Transaction on Systems, Man, and Cybernetics SMC-11(6), June 1981.
19) Paul, R. P. C., Shimano, B., "Compliance and Control", In Proceedings of the Joint Automatic Control Conference, pages 694-699. San Francisco, 1976.
20) Raibert, M. H., Craig, J. J., "Hybrid Position/Force Control of Manipulators", ASME Journal of Dynamic Systems, Measurement, and Control 102:126-133, June, 1981.
21) Safonov, M. G., "Athans, M., Gain and Phase Margin for Multiloop LQG Regulators", IEEE Transaction on Automatic Control AC-22(2):173-179, April, 1977.
22) Salisbury, K. J., "Active Stiffness Control of Manipulator in Cartesian Coordinates", In Proceedings of the 19th IEEE CDC, Albuquerque, New Mexico, December, 1980.
23) Slotine, J. J. , "Sliding Controller Design for Non-linear Systems", International Journal of Control, V40, N2, 84.
24) Slotine, J. J., "The robust Control of of Robot Manipulators", The international Journal of Robotics Research, V4, N2, 1985.
25) Vidyasagar, M., "Nonlinear Systems Analysis", Prentice-Hall.
26) Vidyasagar, M., Desoer, C. A., " Feedback Systems: Input-Output Properties", Academic Press.
27) Vidyasagar, M., Spong, M. W., "Robust Nonlinear Control of Robot Manipulators", IEEE Conference on Decision and Control", December 1985.
28) Whitney, D. E., "Force-Feedback Control of Manipulator Fine Motions", ASME Journal of Dynamic Systems, Measurement, and Control :91-97, June, 1977.